Electronic Supplementary Material (ESI) for CrystEngComm

Supporting Information

High Energy Explosive with Low Sensitivity: A New Energetic Cocrystal Based on CL-20 and BMDNP

Suming Jing*[a] , Jiahao Deng[a] ,Cong Li[a] ,Jin Zhu[a],Yucun Liu [a], Yuanyuan Wang [a] ,Wei Zhang [b] , Jia Liu[c]

[a] College of Environmental and Safety Engineering, North University of China, Taiyuan 030051, China.

[b] Shanxi Jiangyang Chemical Plant.

[c] Hubei Sanjiang Aerospace Jianghe Chemical Technology Co, Ltd.

Contents

SI 1. Single Crystal X-ray Diffraction (SXRD)

The single crystal X-ray diffraction data of the cocrystal were collected using a Rigaku XtaLAB-Synergy-S diffractometer in Japan with Cu-Kα radiation (λ= 1.54184 Å). During data collection, the crystal was kept at 298 K. Data were processed using Olex2 software. The data were solved and optimised using SHELXL. The single crystal structure and optimized structure is shown in Figure S1, S2, and the bond lengths, bond angles, and optimized coordinates of the cocrystal are shown in Table 1,2,3. Information about hydrogen bonding is shown in Table 4.

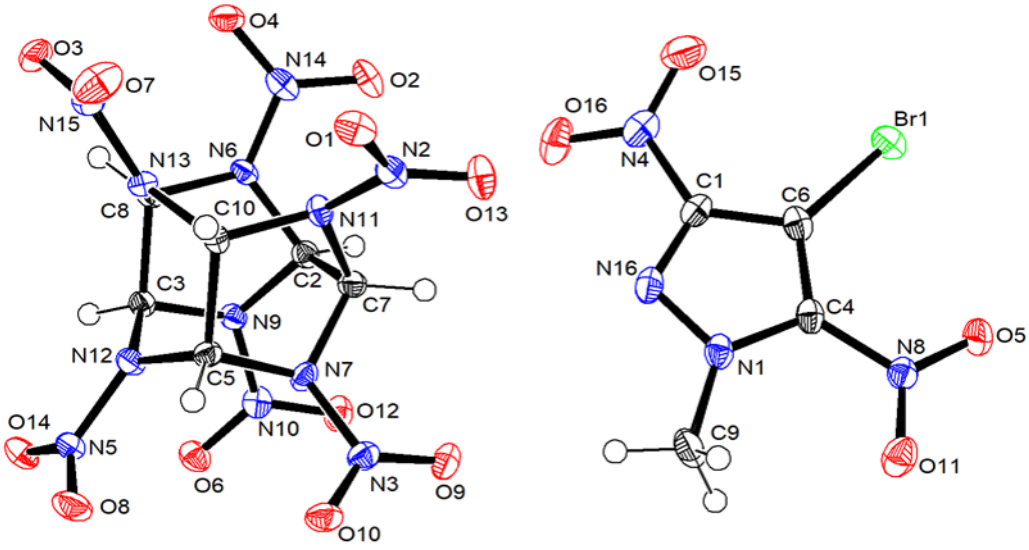

Figure. S1 Ortep diagram for the CL-20/BMDNP cocrystal with 50% probability ellipsoids.

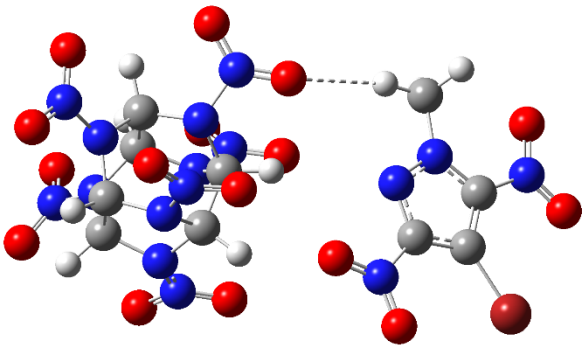

Figure. S2 Optimized structure by Gaussian 09 software.

Table 1. Bond lengths(Å) for Cl-20/BMDNP cocrystal.

Bond	Bond lengths	Bond	Bond lengths
Br1-C6	1.861(4)	O13-N2	1.216(4)
O5-N8	1.222(4)	O14-N5	1.210(4)
O11-N8	1.230(4)	N2-N11	1.415(4)
O15-N4	1.227(5)	N3-N7	1.411(4)
O16-N4	1.222(4)	N5-N12	1.400(4)
N1-N16	1.327(4)	N6-N14	1.361(4)
N1-C4	1.359(5)	N6-C2	1.456(5)
N1-C9	1.457(5)	N6-C8	1.473(4)
N4-C1	1.449(5)	N7-C5	1.469(4)
N8-C4	1.448(5)	N7-C7	1.465(5)
N16-C1	1.315(5)	N9-N10	1.371(4)
C1-C6	1.399(5)	N9-C2	1.449(4)
C4-C6	1.369(6)	N9-C3	1.478(4)
O1-N2	1.216(4)	N11-C7	1.458(5)
O2-N14	1.231(4)	N11-C10	1.473(4)
O3-N15	1.217(4)	N12-C3	1.433(4)
O4-N14	1.223(4)	N12-C5	1.453(4)
O6-N10	1.222(4)	N13-N15	1.401(4)
O7-N15	1.214(4)	N13-C8	1.438(4)
O8-N5	1.229(4)	N13-C10	1.438(4)
O9-N3	1.222(4)	C2-C7	1.596(5)
O10-N3	1.211(4)	C3-C8	1.574(5)
O12-N10	1.229(4)	C5-C10	1.569(5)

Table 2. Bond angles (°) for Cl-20/BMDNP cocrystal.

Bond	Bond angles	Bond	Bond angles
N16-N1-C4	110.7(3)	O6-N10-O12	127.2(3)
N16-N1-C9	118.5(3)	O6-N10-N9	116.4(3)
C4-N1-C9	130.8(3)	O12-N10-N9	116.4(3)
O15-N4-C1	117.9(3)	N2-N11-C7	119.1(3)
O16-N4-O15	124.4(4)	N2-N11-C10	118.2(3)
O16-N4-C1	117.7(3)	C7-N11-C10	108.6(3)
O5-N8-O11	125.3(3)	N5-N12-C3	119.7(3)
O5-N8-C4	116.7(3)	N5-N12-C5	119.1(3)
O11-N8-C4	118.0(3)	C3-N12-C5	117.8(3)
C1-N16-N1	105.3(3)	N15-N13-C8	120.4(3)
N16-C1-N4	118.5(3)	N15-N13-C10	119.6(2)
N16-C1-C6	113.1(3)	C8-N13-C10	117.4(3)
C6-C1-N4	128.4(3)	O2-N14-N6	116.5(3)
N1-C4-N8	122.3(3)	O4-N14-O2	126.8(3)
N1-C4-C6	108.6(3)	O4-N14-N6	116.7(3)
C6-C4-N8	129.1(3)	O3-N15-N13	116.4(3)
C1-C6-Br1	128.3(3)	O7-N15-O3	127.3(3)
C4-C6-Br1	129.3(3)	O7-N15-N13	116.3(3)
C4-C6-C1	102.2(3)	N6-C2-C7	112.3(3)
O1-N2-N11	115.8(3)	N9-C2-N6	95.1(2)
O13-N2-O1	127.6(3)	N9-C2-C7	113.6(3)
O13-N2-N11	116.4(3)	N9-C3-C8	101.0(3)
O9-N3-N7	115.1(3)	N12-C3-N9	113.6(3)
O10-N3-O9	127.4(3)	N12-C3-C8	108.1(3)
O10-N3-N7	117.2(3)	N7-C5-C10	104.4(3)
O8-N5-N12	116.3(3)	N12-C5-N7	109.6(3)
O14-N5-O8	126.8(3)	N12-C5-C10	108.2(3)
O14-N5-N12	116.9(3)	N7-C7-C2	107.0(3)
N14-N6-C2	119.8(3)	N11-C7-N7	104.0(3)
N14-N6-C8	120.4(3)	N11-C7-C2	107.5(3)
C2-N6-C8	111.8(3)	N6-C8-C3	101.2(2)
N3-N7-C5	118.2(3)	N13-C8-N6	112.2(2)
N3-N7-C7	119.0(3)	N13-C8-C3	108.9(3)
C7-N7-C5	108.8(3)	N11-C10-C5	104.4(3)
N10-N9-C2	119.3(3)	N13-C10-N11	110.7(3)
N10-N9-C3	119.9(3)	N13-C10-C5	108.6(3)
C2-N9-C3	111.7(3)		

Table 3. Fractional Atomic Coordinates (Å×10^4) for CL-20/BMDNP cocrystal.

Atom	x	y	z	Atom	x	y	z
Br1	10924.3(4)	2738.4(3)	544.9(3)	O12	9031(3)	4967(2)	8693(3)
O5	12461(3)	4951(2)	232(3)	O13	5850(3)	4786(3)	3455(3)
O11	11962(3)	6497(2)	1191(3)	O14	5101(3)	6594(2)	10786(2)
O15	8300(3)	2107(3)	2150(3)	N2	4809(3)	5024(2)	4050(3)
O16	8017(3)	2873(3)	4083(3)	N3	7331(3)	6950(3)	6384(3)
N1	10104(3)	5425(3)	2741(3)	N5	4994(3)	6879(3)	9605(3)
N4	8502(3)	2856(3)	2982(3)	N6	5285(3)	3500(2)	7434(3)
N8	11818(3)	5500(3)	1010(3)	N7	6509(3)	6087(2)	6873(3)
N16	9219(3)	4726(3)	3272(3)	N9	6700(3)	4554(2)	8728(3)
C1	9357(4)	3792(3)	2629(3)	N10	7933(3)	5098(3)	9273(3)
C4	10804(4)	4922(3)	1772(3)	N11	5014(3)	4935(2)	5488(3)
C6	10336(4)	3854(3)	1650(3)	N12	4926(3)	6045(2)	8623(3)
C9	10173(4)	6554(3)	3235(4)	N13	3300(3)	4809(2)	7132(3)
O1	3580(3)	5259(2)	3552(3)	N14	4828(3)	2757(3)	6446(2)
O2	5730(3)	2479(2)	5684(2)	N15	1836(3)	4521(2)	6765(3)
O3	1330(3)	3832(2)	7473(3)	C2	6639(4)	4103(3)	7366(3)
O4	3579(3)	2414(2)	6430(2)	C3	5249(3)	4933(3)	9035(3)
O6	7828(3)	5640(2)	10299(2)	C5	5033(3)	6334(3)	7211(3)
O7	1204(3)	5006(3)	5797(3)	C7	6488(4)	5015(3)	6196(3)
O8	4903(3)	7827(2)	9172(2)	C8	4214(4)	4151(3)	8093(3)
O9	8469(3)	6669(2)	5959(2)	C10	4012(4)	5543(3)	6277(3)
O10	6899(2)	7879(2)	6524(2)				

Table 4. Bond lengths(Å) and bond angles (°) of hydrogen bonds.

Interaction	Bond lengths	Bond angles
C9-H9A-O3	2.4022	131.662
C9-H9C-O9	2.2966	172.134
C8-H8-O5	2.5305	106.053
C10-H10-O2	2.4990	116.252
C3-H3-O5	2.4941	107.232
C3-H3-O8	2.5543	116.141

SI 2. Hirshfeld Surface and Interactions

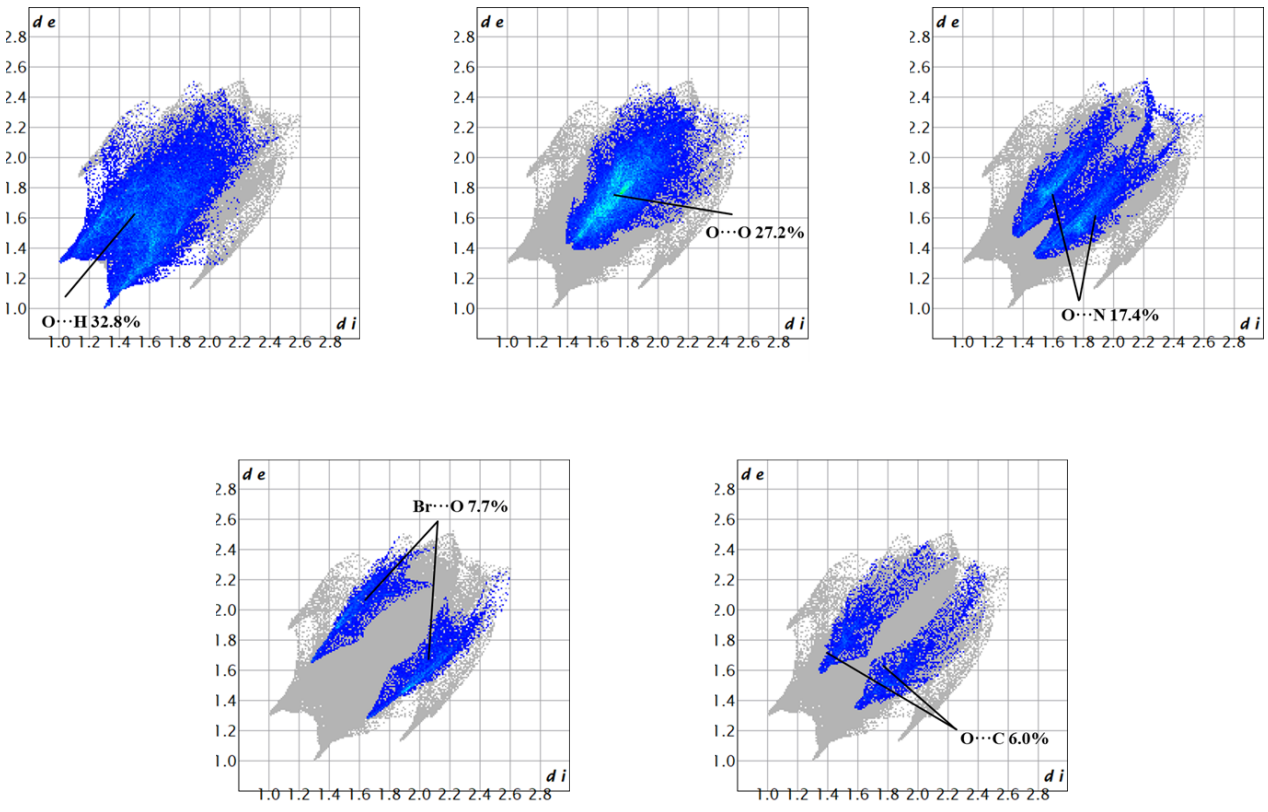

（a）

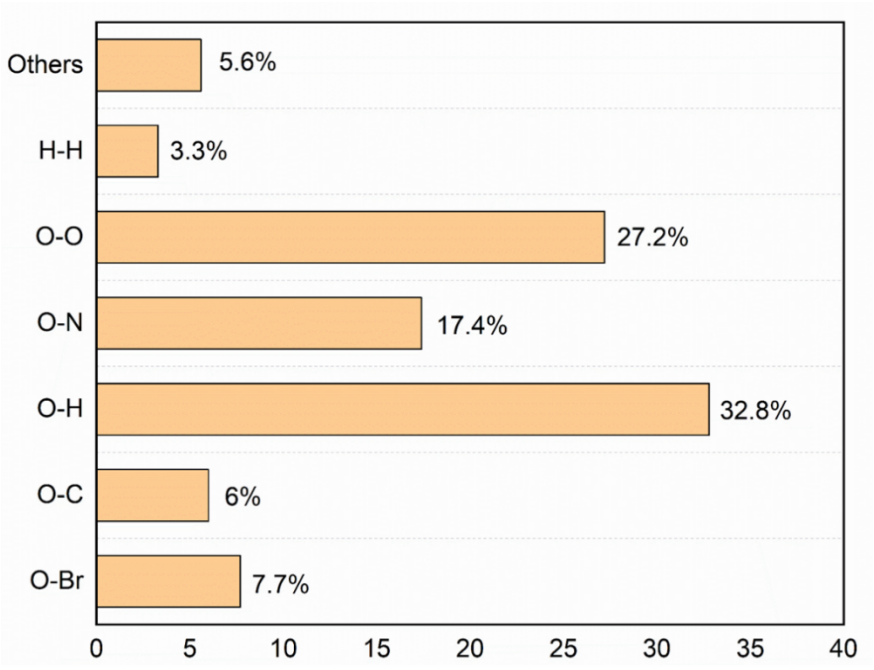

（b）

Figure. S3 Hirshfeld surface and atom contacts of cocrystals: (a)Hirshfeld surface of CL-20/BMDNP

cocrystal, (b) The close contacts percentage contribution to the Hirshfeld surface.

To further explore the cocrystal structure, the 2D fingerprint plots are carried out via Crystal Explorer 3.0 [1-2]. As shown in Figure S3, CL-20/BMDNP cocrystal has the O---H, O---O, O---N, O---C, and Br---O contacts .Among them, the proportion of O-H contacts is 32.8%, confirming the presence of hydrogen bonding interactions; O-N and O-C contacts co-occur in 23.4% of the Hirshfeld surface, indicating the presence of NO2-π interactions. Remarkably, the proportion of O-Br occupies 7.7% of the Hirshfeld surface, suggesting that the weak intermolecular interaction force similar to hydrogen bonding, which is a halogen bond formed by the halogen element Br with O atoms, also plays a role in the process of cocrystal formation.

SI 3. Detonation property evaluation

The Gaussian 09 software [3-4] was used to optimize the cocrystal structure and the Explo5 program [5] was used to predict the detonation characteristics of the cocrystal molecules such as detonation velocity and detonation pressure.

In this paper, the crystal densities in Crystallographic Information Files (CIFs) files are used, and the solid-phase generation enthalpy $\Delta H_{f,\,solid}$ from Gaussian 09 simulation results is used as the theoretical generation enthalpy, and the Explo5 program is used for the calculation of the detonation properties. Among them, the solid-phase generation enthalpy of cocrystal molecules was calculated by Gaussian 09 through the DFT-B3PW91 method, optimised under the 6-31G (d, p) basis group.

According to Hess's law, the enthalpy of solid-phase formation is represented by the enthalpy of gas-phase formation and the enthalpy of sublimation as shown in Equation 1：

$$\Delta H_{f,\,solid} = \Delta H_{f,\,gas} - \Delta H_{sub} \tag{1}$$

where the enthalpy of sublimation can be calculated by the method proposed by Politzer [6], based on the molecular surface area of the energy-containing compound (A), the electrostatic interaction index ($\nu\sigma_{tot}^{2}$) and the correlation coefficient determined by Rice [7], as shown in Equation 2：

$$\Delta H_{sub} = 0.000267\mathrm{A}^2 + 1.65(\nu\sigma_{tot}^{2})^{0.5} - 2.966078 \tag{2}$$

The gas phase enthalpy of formation ($\Delta H_{f,\,gas}$) can be predicted for target compounds based on isobonding reactions. The isobonding reaction profile is shown in Equation 3 and 4. Some of the data described above are presented in the Table 5 and 6.

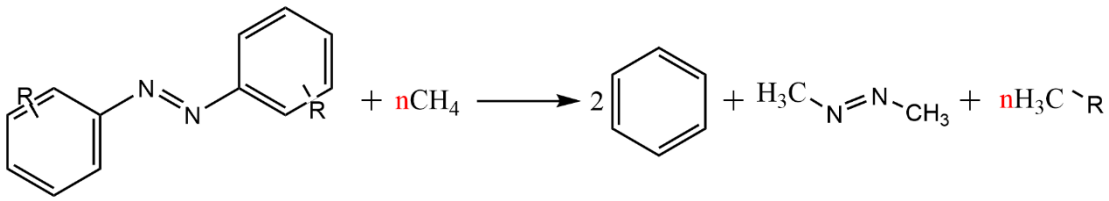

$$\Delta_r H_{298} = \Delta E_0 + \Delta ZPE + \Delta H_T + \Delta(pV) \tag{3}$$

$$\Delta_r H_{298} = \sum \Delta H_{f,gas,P} + \sum \Delta H_{f,gas,R} \tag{4}$$

In Equation 3 and 4: $\Delta E_0$is the value of the total energy change between the product and the reactant at 0 K; ΔZPE is the value of the zero-point energy change between the product and the reactant; ΔH_T is the value of the change of the thermal correction value before and after the reaction; P denotes the product and R denotes the reactant.

Table 5. Relevant data results calculated by the Multiwfn programme.

Item	Results
Volume	548.98520 Å^3
Estimated density according to mass and volume (M/V)	2.0846 g/cm^3
Overall surface area	469.98319 Å^2
Positive surface area	251.44445 Å^2
Negative surface area	218.53873 Å^2
Overall variance (sigma^2_tot)	174.21158 (kcal/mol)^2
Balance of charges (nu)	0.12213586
Product of sigma^2_tot and nu	21.27748 (kcal/mol)^2

Table 6. Theoretical calculation of partial data.

ρ(g·cm^3)	A	$\nu\sigma_{tot}^2$	$\Delta H_{f,\ gas}$(kj·mol^{-1})	ΔH_{sub}(kj·mol^{-1})	$\Delta H_{f,\ solid}$(kj·mol^{-1})
2.081	469.98	21.27728	1126.76578	69.5535	1057.76578

Table 7. Predicted detonation performances of cocrystals, raw materials and references

Samples	Density (g·cm^3)	Detonation velocity （m/s）	Detonation pressure (GPa)
CL-20	2.035	9792	45.07
BMDNP	2.13	6647	22.74
Cocrystal	2.081	8847	38.97
HMX	1.900	9214	38.58
RDX	1.816	8877	34.94
CL-20/TNT	1.846	8558	32.69

For comparisons, CL-20, BMDNP, HMX, RDX, CL-20/TNT and cocrystal were also calculated by the same method.

SI 4. References

[1] J. J. McKinnon, D. Jayatilaka, M. A. Spackman, Towards quantitative analysis of intermolecular interactions with Hirshfeld surfaces, Chem. Commun., 2007, 37, 3814-3816

[2] M. A. Spackman, D. Jayatilaka, Hirshfeld surface analysis, CrystEngComm, 2009, 11, 19 32.

[3] Becke, A. D. (1992). Density‐functional thermochemistry. I. The effect of the exchange‐only gradient correction. The Journal of chemical physics, 96(3), 2155-2160.

[4] Lu T, Chen F. Multiwfn: A multifunctional wavefunction analyzer[J]. Journal of computational chemistry, 2012, 33(5): 580-592.

[5] Sućeska M. EXPLO5–Computer program for calculation of detonation parameters[C]//Proc. of 32nd Int. Annual Conference of ICT, Karlsruhe, Germany. 2001, 110: 1-13.

[6] Politzer P, Murray J S. Some perspectives on estimating detonation properties of C, H, N, O compounds[J]. Central European Journal of Energetic Materials, 2011, 8(3): 209-220.

[7] Byrd E F C, Rice B M. Improved prediction of heats of formation of energetic materials using quantum mechanical calculations[J]. The Journal of Physical Chemistry A, 2006, 110(3): 1005-1013.